Intrinsic ripples in graphene

A. FASOLINO*, J. H. LOS AND M. I. KATSNELSON

Institute for Molecules and Materials, Radboud University Nijmegen, Toernooiveld 1, 6525ED Nijmegen, The Netherlands

*e-mail: a.fasolino@science.ru.nl

Published online: 23 September 2007; doi:10.1038/nmat2011

The stability of two-dimensional (2D) layers and membranes is the subject of a long-standing theoretical debate. According to the so-called Mermin–Wagner theorem[1], long-wavelength fluctuations destroy the long-range order of 2D crystals. Similarly, 2D membranes embedded in a 3D space have a tendency to be crumpled[2]. These fluctuations can, however, be suppressed by anharmonic coupling between bending and stretching modes meaning that a 2D membrane can exist but will exhibit strong height fluctuations[2–4]. The discovery of graphene, the first truly 2D crystal[5,6], and the recent experimental observation of ripples in suspended graphene[7] make these issues especially important. Besides the academic interest, understanding the mechanisms of the stability of graphene is crucial for understanding electronic transport in this material that is attracting so much interest owing to its unusual Dirac spectrum and electronic properties[8–11]. We address the nature of these height fluctuations by means of atomistic Monte Carlo simulations based on a very accurate many-body interatomic potential for carbon[12]. We find that ripples spontaneously appear owing to thermal fluctuations with a size distribution peaked around 80 Å which is compatible with experimental findings[7] (50–100 Å). This unexpected result might be due to the multiplicity of chemical bonding in carbon.

The phenomenological theories for flexible membranes[2–4] are derived in the continuum limit without including any microscopic feature and their applicability to graphene in the interesting range of temperatures, sample sizes and so on is not evident. We present Monte Carlo simulations of the equilibrium structure of single-layer graphene. By monitoring the normal–normal correlation functions, we can directly compare our results with the predictions of the existing theories. The effect of interest is crucially dependent on acoustical phonons and interactions between them and therefore the simulations require samples much larger than interatomic distances, making *ab initio* Car–Parrinello[13] simulations prohibitive. However, for carbon a very accurate description of the energetic and thermodynamic properties of different phases is provided by the effective many-body potential LCBOPII (refs 12,14). This bond-order potential is constructed in such a way as to provide a unified description of the energetics and elastic constants of all carbon phases as well as the energy characteristics of different defects with accuracy comparable to experimental accuracy. We find clear deviations from harmonic behaviour for long-wavelength fluctuations and an interesting and unexpected maximum of fluctuations with wavelength of about 80 Å. We relate these features to fluctuations in bond length that in carbon signal a change from conjugated to single/double bonds, with consequent deviations from planarity.

We carry out atomistic Monte Carlo simulations based on the standard Metropolis algorithm for approximately squared samples of different sizes (see Table 1) with periodic boundary conditions. Monte Carlo simulations yield static equilibrium properties as ensemble averages in the canonical ensemble, whereas molecular dynamics yields the same quantities as time averages. For ergodic systems, the two approaches are equivalent[15]. However, Monte Carlo needs only energy evaluations, which are computationally much cheaper than the force evaluations needed in molecular dynamics. Moreover, the Metropolis algorithm[15] provides a very efficient way to generate configurations for averaging in accord with the Boltzmann distribution, avoiding wasting time with the astronomical number of configurations of low statistical weight. We always start with completely flat graphene layers to avoid any bias. Typically we used 400,000 Monte Carlo steps (1 Monte Carlo step corresponds to N attempts to a coordinate change) to thermalize and 500,000 Monte Carlo steps for averaging. Every 5 Monte Carlo steps, we allow for isotropic size fluctuations of the box. We have checked that the results remain basically the same if anisotropic size fluctuations are allowed. The energy of a given configuration is evaluated according to the bond-order potential LCBOPII developed recently[12]. This potential is based on a large database of experimental and theoretical data for molecules and solids and has been proved to describe very well thermodynamic and structural properties of all phases of carbon and its phase diagram in a wide range of temperatures and pressures[12,14]. We believe that LCBOPII can give a good description of graphene because it correctly reproduces its elastic properties and yields the structure and energetics of vacancies in graphene in good agreement with *ab initio* calculations[16]. Of particular importance here is the fact that bond-order potentials correlate coordination, bond length and bond strength, allowing changes between single, double and conjugated bonds with the correct energetics. Most simulations have been carried out at room temperature, $T = 300$ K, but we have also simulated some of the structures at high temperature, $T = 1{,}000$, 2,000 and 3,500 K.

A typical configuration of graphene at room temperature is shown in Fig. 1. The first thing to note is that height fluctuations are present at equilibrium. We find a very broad distribution of height displacements, $\bar{h}$, with a typical size of the order of 0.7 Å for the $N = 8{,}640$ sample, comparable to the interatomic distance 1.42 Å. In all of our simulations we have never observed any topological defect, such as the Stone–Wales 5–7–7–5 rings that could provide an alternative source of corrugation, as expected from their high formation energy[12]. Indeed, no experimental evidence of their existence has been reported either[7].

The natural way to further analyse our results is to compare them with the results and predictions of the phenomenological

Table 1 Details of the simulated samples. The initial, roughly squared, box is defined by $(L_x, L_y) = (p|a_1|, q|a_1 - 2a_2|)$, where a_1 and a_2 are the in-plane lattice vectors $a_1 = a\sqrt{3}x$, $a_2 = a((\sqrt{3}/2)x + (3/2)y)$, with x and y being cartesian unit vectors.

N	p	q	L_x (Å)	L_y (Å)
240	10	6	24.59	25.56
960	20	12	49.29	51.12
2,160	30	18	73.78	76.68
4,860	45	27	110.68	115.02
8,640	60	36	147.57	153.36
12,096	72	42	177.08	178.92
19,940	90	54	221.36	230.04

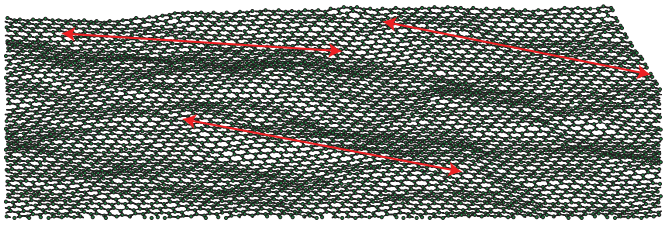

Figure 1 A representative configuration of the $N = 8{,}640$ sample at $T = 300$ K. The red arrows are ~80 Å long.

theories of thermal fluctuations in flexible membranes[2–4] reviewed in more detail in the Supplementary Information. The primary quantities are the two-component displacement vector in the plane **u**, the out-of-plane displacement h and the normal unit vector **n** with in-plane component $-\nabla h/\sqrt{1+(\nabla h)^2}$ (see the schematic diagram in Supplementary Information, Fig. S1).

In harmonic approximation, the bending (h) and stretching (**u**) modes are decoupled. In this approximation, it can be shown that the Fourier components of the bending correlation function with wavevector **q** are[2]

$$\langle |h_{\mathbf{q}}|^2 \rangle = \frac{TN}{\kappa S_0 q^4},$$

where N is the number of atoms, κ is the bending rigidity, $S_0 = L_x L_y/N$ is the area per atom and T is the temperature in units of energy. The mean-square displacement in the direction normal to the layer becomes

$$\langle h^2 \rangle = \sum_{\mathbf{q}} \langle |h_{\mathbf{q}}|^2 \rangle \propto \frac{T}{\kappa} L^2, \qquad (1)$$

where L is a typical linear sample size. In the harmonic approximation, the correlation function of the normals

$$G(q) = \langle |\mathbf{n}_{\mathbf{q}}|^2 \rangle = q^2 \langle |h_{\mathbf{q}}|^2 \rangle$$

becomes

$$G_0(q) = \frac{TN}{\kappa S_0 q^2}, \qquad (2)$$

which implies that the mean-square angle between the normals is logarithmically divergent as $L \to \infty$ (ref. 2). This behaviour corresponds to the tendency for crumpling of membranes due to thermally excited harmonic phonons.

Deviations from this harmonic behaviour due to anharmonic coupling between bending and stretching modes can stabilize the flat phase by suppressing the long-wavelength fluctuations[2–4]. In this case, the corresponding correlation function of the normals is given by the Dyson equation

$$G_a^{-1}(q) = G_0^{-1}(q) + \Sigma(q) \qquad (3)$$

with self-energy

$$\Sigma(q) = \frac{AS_0}{Nq^2}\left(\frac{q}{q_0}\right)^{\eta}, \qquad (4)$$

where $q_0 = 2\pi\sqrt{B/\kappa}$, with B being the two-dimensional bulk modulus ($B = 0.4\,\mathrm{eV\,Å^{-2}}$ at $T = 0$ according to LCBOPII), η being the anomalous rigidity exponent and A being an unknown numerical factor. Self-consistent perturbation theory[4] gives $\eta \approx 0.8$. As a result of this anharmonic coupling, the typical height of the fluctuations in the direction normal to the membrane is much smaller than the one given by equation (1) and scales with the sample size as L^{ζ}, with $\zeta = 1 - \eta/2$. Nevertheless, the fluctuations are still anomalously large and they can be much larger than the interatomic distance for large samples. Thus, the theory predicts an intrinsic tendency for ripple formation. At the same time, the amplitude, $\overline{h} \propto L^{\zeta}$, of these transverse fluctuations remains much smaller than the sample size and preserves the long-range order of the normals so that the membrane can be considered as approximately flat and not crumpled.

To obtain a quantitative comparison with these theoretical predictions for the spatial distribution of the ripples, we have calculated numerically the Fourier components of the correlation function of the normals, $G(q)$, for q_x and q_y multiples of $2\pi/L_x$ and $2\pi/L_y$ respectively.

The Ginzburg criterion[2] gives an approximate value of the wavevector of the fluctuations, q^*, and thus the spatial scale, $L^* = 2\pi/q^*$, at which anharmonic corrections become dominant as

$$q^* = \sqrt{\frac{3TB}{8\pi\kappa^2}} \qquad (5)$$

(for derivation see the Supplementary Information).

For graphene at room temperature, this estimate gives $L^* \approx 200$ Å so that only studies of samples larger than L^* could possibly access the anharmonic regime. The large value of L^* results from the smallness of the ratio T/κ (1/40 at room temperature) owing to the strong chemical bond in graphene. Therefore, for the realistic representation of carbon bonding and the sample sizes studied here, we can expect to observe modest anharmonic corrections to the leading harmonic terms. Conversely, simulations of model-tethered membranes with $\kappa/T \approx 1$ could easily reach sample sizes suitable to access the long-wavelength regime and estimate the exponent $\eta \approx 0.6$–0.8 (refs 17,18).

Figure 2a shows $G(q)$ at $T = 300$ K for several samples. As expected, there is a whole range of wavevectors where the harmonic approximation given by equation (2) is quite accurate. The rigidity $\kappa = 1.1$ eV extracted from the data at $T = 300$ K by comparison with equation (2) is in very good agreement with the experimental value of 1.2 eV derived from the phonon spectrum of graphite[19]. As q decreases, we observe deviations from harmonic behaviour in good agreement with equations (3) and (4). However, at smaller q, the behaviour of $G(q)$ is no longer described by the harmonic approximation $G_0(q)$ or by the anharmonic expression $G_a(q)$. In this region, the most remarkable feature of $G(q)$ is a maximum instead of the power-law dependence $G_a(q)$ that implies the absence of any relevant length scale in the system. The presence of

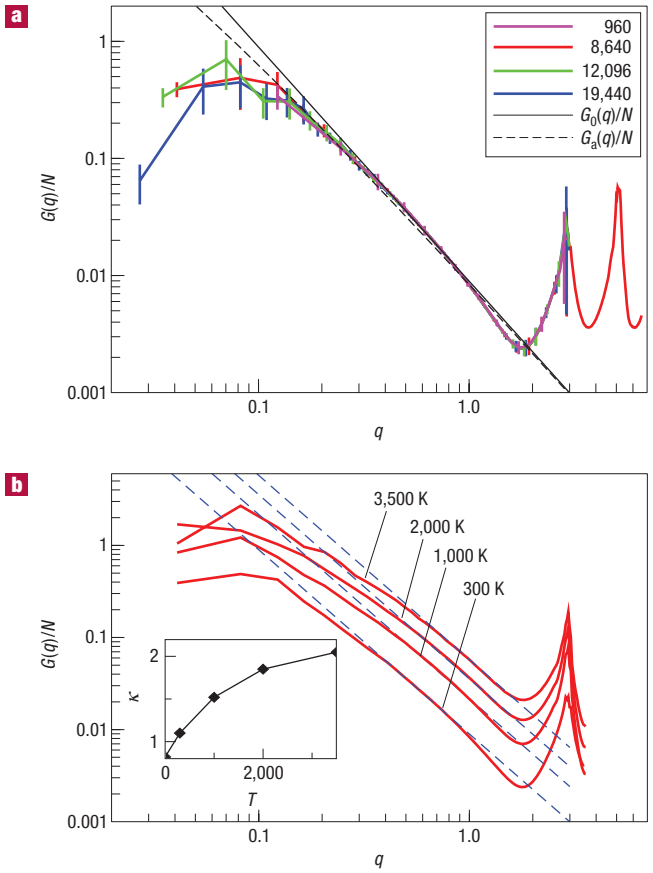

Figure 2 Fourier transform of the correlation function of the normals. **a**, Normal–normal correlation function, $G(q)/N$, for some of the studied samples at $T = 300$ K. The solid straight line gives the harmonic power-law behaviour $G_0(q)/N$ (equation (2)) with $\kappa = 1.1$ eV and the dashed line gives $G_a(q)/N$ (equations (3) and (4)) with $A = 1$, $\eta = 0.8$. Deviations from harmonic behaviour occur for q close to the Bragg peaks at $q = 4\pi/3a = 2.94$ Å^{-1} and $q = 4\pi/\sqrt{(3)}a = 5.11$ Å^{-1} with $a = 1.42$ Å and at small q. The maximum of $G(q)$ at $q \approx 0.08$ Å^{-1} signals a preferred length scale of about 80 Å. **b**, $G(q)/N$ for the $N = 8{,}640$ sample at the indicated temperatures. The dashed lines give the harmonic power-law behaviour $G_0(q)$ with $\kappa = 1.1$, 1.52, 1.85 and 2.05 eV at $T = 300$, 1,000, 2,000 and 3,500 K respectively, which are plotted in the inset. The $T = 0$ value $\kappa = 0.82$ eV is found by direct total energy calculations.

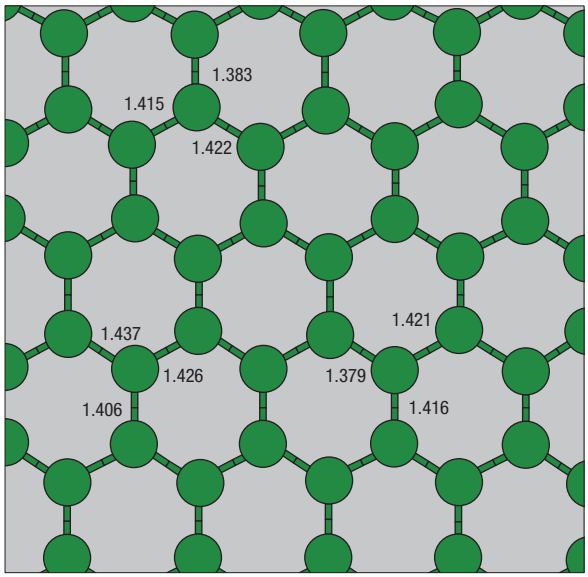

Figure 3 Portion of one typical configuration of the $N = 8{,}640$ sample at $T = 300$ K. The numbers indicate the bond length in Å. Note that often one of the bonds with the first neighbours is much shorter than the other two.

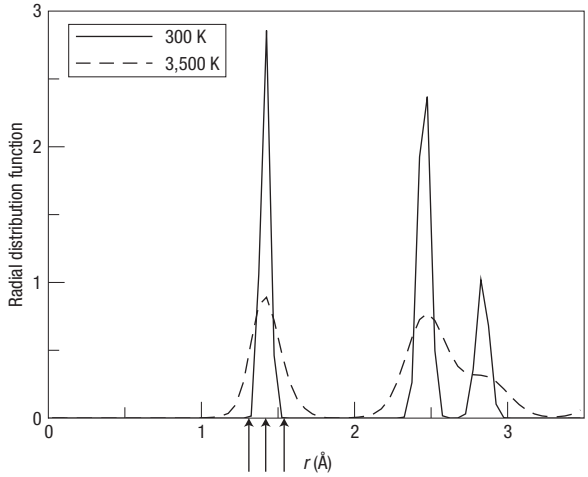

Figure 4 Radial distribution function for the $N = 8{,}640$ sample at $T = 300$ K and $T = 3{,}500$ K as a function of interatomic distance. The arrows indicate the length of double ($r = 1.31$ Å), conjugated ($r = 1.42$ Å) and single ($r = 1.54$ Å) bonds.

this maximum instead, means that there is a preferred average value of about 80 Å as shown by the arrows in Fig. 1.

These results are also confirmed at higher temperatures. Figure 2b shows the results at four temperatures for the $N = 8{,}640$ sample. The fit of the results in the harmonic regime yields the temperature dependence of κ that increases to $\kappa \approx 2.0$ eV at $T = 3{,}500$ K.

The preferable length that we find is reminiscent of the 'avoided criticality' scenario in frustrated systems near second-order phase transitions[20]. Such systems have an intrinsic tendency to be modulated and to form some inhomogeneous patterns that destroy the scaling. It is known that some soft condensed-matter membranes have a tendency for spontaneous bending and ripple formation[21–23], but this behaviour for elemental solids such as graphene is unexpected.

This is probably due to the peculiar character of bonding in carbon. In the ground state of graphene all bonds are equivalent (conjugated bonds). However, even at room temperature, there is a large probability of having an asymmetric distribution of short/long (double/single) bonds, implying deviations from planarity (see Fig. 3). Indeed, the radial distribution functions shown in Fig. 4 for two temperatures show an anomalously broad distribution of first-neighbour bond lengths, going down to the length of double bonds in carbon of 1.31 Å even at $T = 300$ K. Changes of bond conjugation are also the reason for the negative thermal expansion coefficient in graphene found in *ab initio* calculations[24]. We also observe a 0.13% contraction of the lattice spacing at $T = 300$ K, in agreement with the 0.11% contraction in ref. 24. We suggest that the ability of carbon to form different types of bond makes graphene different from a generic two-dimensional crystal.

The results obtained are relevant not only for a better understanding of the stability and structure of graphene but also of electronic transport. The fluctuations of the normals lead to a modulation of the hopping integrals and are bound to affect the electronic structure. In particular, suppression of weak localization[25], modulation of the electrostatic potential[26] and essential contributions to charge-carrier scattering[27] have been discussed. Knowledge of the normal–normal correlation functions is necessary for the calculation of the electron scattering by ripples.

The cleavage technique that has led to the discovery of graphene has already been applied to other layered materials, such as BN[5], so the investigation of structural properties of 1-atom-thick layers is important for a whole new class of systems. It will be very instructive to carry out systematic experimental and theoretical investigations of other two-dimensional crystals to understand which properties are common to flexible membranes and which are consequences of particular features of the chemical bonding and interatomic interactions.

Received 16 April 2007; accepted 16 August 2007; published 23 September 2007.

References

1. Mermin, N. D. Crystalline order in two dimensions. *Phys. Rev.* **176**, 250–254 (1968).
2. Nelson, D. R., Piran, T. & Weinberg, S. (eds) *Statistical Mechanics of Membranes and Surfaces* (World Scientific, Singapore, 2004).
3. Nelson, D. R. & Peliti, L. Fluctuations in membranes with crystalline and hexatic order. *J. Physique* **48**, 1085–1092 (1987).
4. Le Doussal, P. & Radzihovsky, L. Self-consistent theory of polymerized membranes. *Phys. Rev. Lett.* **69**, 1209–1212 (1992).
5. Novoselov, K. S. *et al*. Two-dimensional atomic crystals. *Proc. Natl Acad. Sci. USA* **102**, 10451–10453 (2005).
6. Novoselov, K. S. *et al*. Electric field effect in atomically thin carbon films. *Science* **306**, 666–669 (2004).
7. Meyer, J. C. *et al*. The structure of suspended graphene membrane. *Nature* **446**, 60–63 (2007).
8. Novoselov, K. S. *et al*. Two-dimensional gas of massless Dirac fermions in graphene. *Nature* **438**, 197–200 (2005).
9. Zhang, Y., Tan, J. W., Stormer, H. L. & Kim, P. Experimental observation of the quantum Hall effect and Berry's phase in graphene. *Nature* **438**, 201–204 (2005).
10. Geim, A. K. & Novoselov, K. S. The rise of graphene. *Nature Mater.* **6**, 183–191 (2007).
11. Katsnelson, M. I. Graphene: Carbon in two dimensions. *Mater. Today* **10**, 20–27 (2007).
12. Los, J. H., Ghiringhelli, L. M., Meijer, E. J. & Fasolino, A. Improved long-range reactive bond-order potential for carbon. I. Construction. *Phys. Rev. B* **72**, 214102 (2005).
13. Car, R. & Parrinello, M. Unified approach for molecular dynamics and density-functional theory. *Phys. Rev. Lett.* **55**, 2471–2474 (1985).
14. Ghiringhelli, L. M., Los, J. H., Meijer, E. J., Fasolino, A. & Frenkel, D. Modeling the phase diagram of carbon. *Phys. Rev. Lett.* **94**, 145701 (2005).
15. Chandler, D. *Introduction to Modern Statistical Mechanics* Chaps 3 and 6 (Oxford Univ. Press, New York, 1987).
16. Carlsson, J. M. & Scheffler, M. Structural, electronic, and chemical properties of nanoporous carbon. *Phys. Rev. Lett.* **96**, 046806 (2006).
17. Bowick, M. J. in *Statistical Mechanics of Membranes and Surfaces* (eds Nelson, D. R., Piran, T. & Weinberg, S.) Ch. 11 (World Scientific, Singapore, 2004).
18. Abramovitz, F. F. & Nelson, D. R. Diffraction from polymerized membranes. *Science* **249**, 393 (1990).
19. Niclow, R., Wakabayashi, N. & Smith, H. G. Lattice dynamics of pyrolytic graphite. *Phys. Rev. B* **5**, 4951–4962 (1972).
20. Tarjus, G., Kivelson, S. A., Nussinov, Z. & Viot, P. The frustrated-based approach of supercooled liquids and the glass transition: A review and critical assessment. *J. Phys. Condens. Matter* **17**, R1143–R1182 (2005).
21. Katsnelson, M. I. & Fasolino, A. Solvent-driven formation of bolaamphiphilic vesicles. *J. Phys. Chem. B* **110**, 30–32 (2006).
22. Manyuhina, O. V. *et al*. Anharmonic magnetic deformation of self-assembled molecular nanocapsules. *Phys. Rev. Lett.* **98**, 146101 (2007).
23. Lubensky, T. C. & MacKintosh, F. C. Theory of "rippled" phases of liquid bilayers. *Phys. Rev. Lett.* **71**, 1565–1568 (1993).
24. Mounet, N. & Marzari, N. First-principles determination of the structural, vibrational and thermodynamic properties of diamond, graphite, and derivatives. *Phys. Rev. B* **71**, 205214 (2005).
25. Morozov, S. V. *et al*. Strong suppression of weak localization in graphene. *Phys. Rev. Lett.* **97**, 016801 (2006).
26. Castro Neto, A. H. & Kim, E. A. Charge inhomogeneity and the structure of graphene sheets. Preprint at <http://arxiv.org/cond-mat/0702562> (2007).
27. Geim, A. K. & Katsnelson, M. I. Electronic scattering on microscopic corrugations in graphene. *Phil. Trans. R. Soc. A* (in the press); preprint at <http://arxiv.org/arXiv:0706.2490> (2007).

Acknowledgements

We are grateful to D. Nelson, J. C. Maan, A. Geim, K. Novoselov and J. Meyer for helpful discussions. This work was supported by the Stichting voor Fundamenteel Onderzoek der Materie (FOM), the Netherlands.
Correspondence and requests for materials should be addressed to A.F.
Supplementary Information accompanies this paper on www.nature.com/naturematerials.